ACS APPLIED MATERIALS & INTERFACES

www.acsami.org

Research Article

# Enzyme- and Relative Humidity-Responsive Antimicrobial Fibers for Active Food Packaging

Zeynep Aytac,[▽] Jie Xu,[▽] Suresh Kumar Raman Pillai, Brian D. Eitzer, Tao Xu, Nachiket Vaze, Kee Woei Ng, Jason C. White, Mary B. Chan-Park, Yaguang Luo, and Philip Demokritou*

Cite This: *ACS Appl. Mater. Interfaces* 2021, 13, 50298–50308

Read Online

ACCESS | Metrics & More | Article Recommendations | Supporting Information

**ABSTRACT:** Active food packaging materials that are sustainable, biodegradable, and capable of precise delivery of antimicrobial active ingredients (AIs) are in high demand. Here, we report the development of novel enzyme- and relative humidity (RH)-responsive antimicrobial fibers with an average diameter of 225 ± 50 nm, which can be deposited as a functional layer for packaging materials. Cellulose nanocrystals (CNCs), zein (protein), and starch were electrospun to form multi-stimuli-responsive fibers that incorporated a cocktail of both free nature-derived antimicrobials such as thyme oil, citric acid, and nisin and cyclodextrin-inclusion complexes (CD-ICs) of thyme oil, sorbic acid, and nisin. The multistimuli-responsive fibers were designed to release the free AIs and CD-ICs of AIs in response to enzyme and RH triggers, respectively. Enzyme-responsive release of free AIs is achieved due to the degradation of selected polymers, forming the backbone of the fibers. For instance, protease enzyme can degrade zein polymer, further accelerating the release of AIs from the fibers. Similarly, RH-responsive release is obtained due to the unique chemical nature of CD-ICs, enabling the release of AIs from the cavity at high RH. The successful synthesis of CD-ICs of AIs and incorporation of antimicrobials in the structure of the multistimuli-responsive fibers were confirmed by X-ray diffraction and Fourier transform infrared spectrometry. Fibers were capable of releasing free AIs when triggered by microorganism-exudated enzymes in a dose-dependent manner and releasing CD-IC form of AIs in response to high relative humidity (95% RH). With 24 h of exposure, stimuli-responsive fibers significantly reduced the populations of foodborne pathogenic bacterial surrogates *Escherichia coli* (by ∼5 log unit) and *Listeria innocua* (by ∼5 log unit), as well as fungi *Aspergillus fumigatus* (by >1 log unit). More importantly, the fibers released more AIs at 95% RH than at 50% RH, which resulted in a higher population reduction of *E. coli* at 95% RH. Such biodegradable, nontoxic, and multistimuli-responsive antimicrobial fibers have great potential for broad applications as active and smart packaging systems.

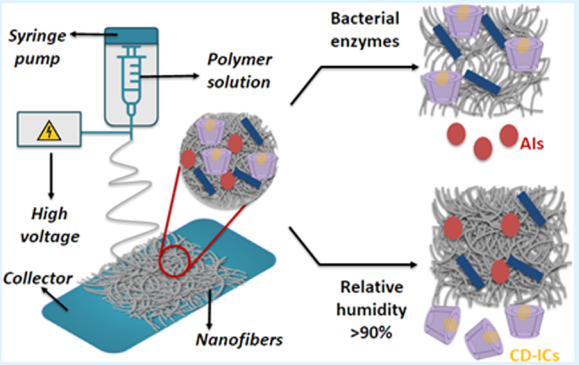


**KEYWORDS:** *electrospinning, sustainable food packaging, cyclodextrin, enzyme, precision agriculture, cellulose nanocrystals, biotic and abiotic-responsive materials*



## INTRODUCTION

Maintaining food safety and security for the increasing global population is one of the most important challenges of the 21st century.[1−3] Food packaging plays a key role in maintaining food safety and quality and can reduce food waste across the "farm to the fork" continuum.[4] Films made of synthetic, petroleum-based polymers are widely used as food packaging materials due to their low cost and excellent gas barrier and mechanical properties.[5] However, films with incorporated antimicrobial active ingredients (AIs) have not been used widely due to their poor antimicrobial performance as a result of the low surface-to-volume ratio and potential negative sensory effects.[6] Advanced fibrous materials with high surface-to-volume ratios are better suited to incorporate minimal quantities of AIs for the development of active, antimicrobial food packaging materials.[7−10] For instance, our group has begun to explore antimicrobial nanofibers using electrospinning of zein and a cocktail of nature-derived antimicrobial agents.[9]

More recently, emphasis has shifted toward the development of "smart" or stimuli-responsive packaging materials to provide precision in the delivery of antimicrobial AIs and minimize the use of chemicals, thereby minimizing sensory and public health concerns. Such advanced materials are designed to exhibit changes in their properties in response to the desired and

Received: June 30, 2021
Accepted: October 1, 2021
Published: October 14, 2021




https://doi.org/10.1021/acsami.1c12319
*ACS Appl. Mater. Interfaces* 2021, 13, 50298−50308

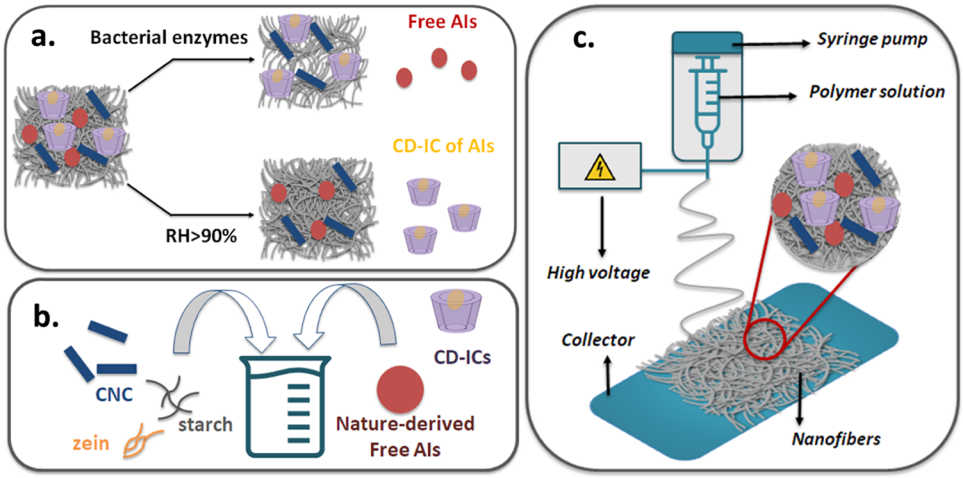


**Figure 1.** (a) Representation of the enzyme- and relative humidity (RH)-triggered strategies; (b) preparation of the solution composed of zein, starch, cellulose nanocrystals (CNCs), nature-derived free active ingredients (AIs), and cyclodextrin-inclusion complexes (CD-ICs) of AIs; and (c) synthesis of multistimuli-responsive fibers by electrospinning.

specific chemical, physical, and biological stimuli such as pH, relative humidity (RH), and enzymes present in the biological exudates secreted by microorganisms.[11] If AIs are incorporated into these responsive materials, such biotic and abiotic stimuli can trigger their release at the right time and at right dose, bringing precision to the delivery.[11]

Here, both biotic (enzymatic) and abiotic (RH) triggers were considered in the design of multistimuli-responsive fibers. More specifically, food-associated microorganisms across various food categories including fresh produce, meat, and bread exude a range of enzymes, including cellulase,[12] protease,[13] and amylase.[14] These enzymes released from various microorganisms can selectively break down specific biopolymers forming the fibers into subunit monomers and trigger the release of antimicrobial AIs to control microbial growth on an as-needed basis.[15] In addition, the sustainable use of such biopolymers for food packaging will also reduce the plastic waste and micro-/nanoplastics environmental crisis caused by synthetic polymers.[5] Furthermore, RH and temperature are key environmental variables related to food safety and quality. The optimum RH for the storage of food categories such as meat and fresh produce is typically above 90%.[16,17] It is also known that foodborne microorganism growth increases as the RH increases above 90%.[18] Therefore, high RH can be used as an abiotic trigger for the release of AIs to prevent microbial growth. For this purpose, compounds named cyclodextrins (CDs) will first encapsulate AIs into their cavity to form cyclodextrin-inclusion complexes (CD-ICs). These CD-ICs of AIs will then be incorporated into the fibers to provide RH responsiveness.

Native CDs are FDA generally recognized as safe (GRAS) compounds and have the ability to make ICs with various types of hydrophobic compounds owing to their relatively hydrophobic cavity. This approach was used to effectively improve the aqueous solubility and thermal stability of a range of analytes.[19] Additionally, such CD-ICs are widely used for biomedical applications such as drug delivery, wound dressing,[20] and tissue engineering.[20,21] It is also known that CD-ICs are disassociated when the RH exceeds 85% as the hydrogen bonds are weakened between the hydrophobic molecules and CD, making this platform an ideal candidate for the triggered release of antimicrobial AIs.[22] It is worth noting that there are only a few published studies on CD-IC applications in food packaging,[8,23,24] focusing on the non-specific delivery of AIs in the absence of a trigger.

In this study, multistimuli-responsive antimicrobial electrospun fibers were developed from cellulose nanocrystals (CNCs), zein, and starch incorporated with nature-derived antimicrobials and their associated CD-ICs. All compounds and solvents used for the fiber "green" synthesis process are FDA-approved GRAS materials to ensure sustainability and scalability. The morphological and physicochemical properties of CD-ICs and fibers, and dissolution kinetics of AIs from fibers in the presence of the RH and enzymatic triggers were assessed using a range of advanced analytical methods. The antimicrobial efficacy of multistimuli fibers was also assessed by standard microbiological methods. The development of such responsive biopolymer-based antimicrobial platforms offers a novel and effective means to promote food shelf life and safety and enhance food security.

## METHODS

Figure 1a–c outlines (1) the enzyme- and RH-triggered strategies; (2), preparation of the polymer solution composed of zein, starch, cellulose nanocrystals (CNCs), nature-derived free active ingredients (AIs), and cyclodextrin-inclusion complexes (CD-ICs) of AIs; and (3) synthesis of multistimuli-responsive fibers by electrospinning.

**Synthesis of CD-ICs of Antimicrobial AIs.** CD-ICs of nature-derived antimicrobial AIs (thyme oil, sorbic acid, nisin) were synthesized using the coprecipitation method. The nature-derived AIs were selected because of their FDA GRAS status and their ability to inactivate a broad range of food-related pathogenic and spoilage microorganisms.[25−27] A schematic representation of the synthesis is given in Figure 2. For γ-CD/thyme oil-IC (1:2) and γ-CD/sorbic acid-IC (1:2), γ-CD (Wacker, Cavamax W8 Food) was first dissolved in water for 10 min, and thyme oil (Sigma-Aldrich, W306509) or sorbic acid (TCI, S0053) was then added into the solution at a 1:2 molar ratio (CD:thyme oil or CD:sorbic acid). For γ-CD/nisin-IC (4:1), γ-CD was dissolved in 5 mL of water for 10 min and was then added into nisin (Alfa Aesar, J66370) that had previously been mixed with a small quantity of thyme oil (15 μL). It is noteworthy that nisin was initially mixed with a small volume of more hydrophobic compound (thyme oil) prior to mixing with γ-CD to further facilitate IC formation. The molar ratio of CD:nisin was 4:1 due to the large molecular weight of nisin compared to that of CD. After stirring the three solutions overnight at room temperature, they were incubated at


https://doi.org/10.1021/acsami.1c12319
ACS Appl. Mater. Interfaces 2021, 13, 50298−50308

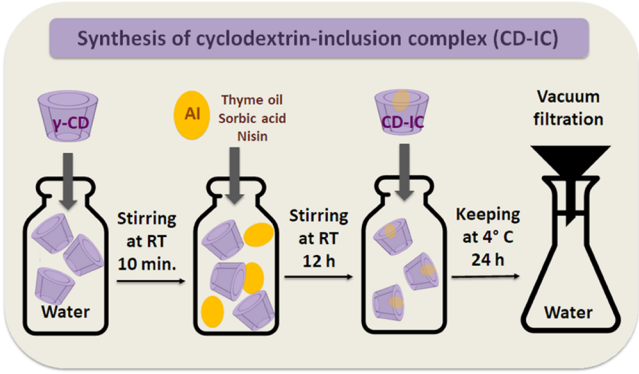


**Figure 2.** Schematic representation of the synthesis of cyclodextrin-inclusion complexes (CD-ICs) of active ingredients (AIs) by a coprecipitation method.

4 °C for 24 h. CD-ICs precipitated at the bottom of the bottle and were collected by vacuum filtration, followed by drying in a hood for 48 h. The resulting solids were ground into fine powders with an agate mortar and pestle.

**Physicochemical Characterization of CD-ICs of AIs.** The crystallinity of γ-CD, γ-CD/thyme oil-IC (1:2), sorbic acid, γ-CD/sorbic acid-IC (1:2), nisin, and γ-CD/nisin-IC (4:1) was investigated by X-ray diffraction (XRD, Bruker D2 Phaser) in the 2θ range of 5−40° using Cu Kα radiation. XRD analysis of thyme oil could not be performed because of its liquid nature. The cage-type crystalline structure of CDs converts to a channel-type crystalline structure when CD-IC is formed. These characteristic peaks of the cage and channel-type crystalline structure allow the determination of successful CD-IC synthesis.[28] The chemical characterization of γ-CD, thyme oil, γ-CD/thyme oil-IC (1:2), sorbic acid, γ-CD/sorbic acid-IC (1:2), nisin, and γ-CD/nisin-IC (4:1) was analyzed using attenuated total reflectance-Fourier transform infrared (ATR-FTIR) spectrometry (Thermo Scientific Nicolet IS50). The spectra were recorded between 4000 and 400 $cm^{-1}$ at a resolution of 4 $cm^{-1}$, and 64 scans/sample were taken.

**"Green" Synthesis of Electrospun Fibers.** *Synthesis of Pristine Fibers (Control Fibers without AIs).* Polymers such as zein, which is a protein, cellulose nanocrystals (CNCs), and starch were chosen to form the backbone of the fiber because enzymes released from bacteria such as protease, amylase, and cellulase will degrade these materials. Acetic acid was used as a solvent for preparing the CNCs, zein, and starch solutions.[29] Finally, in contrast to toxic organic solvents usually preferred in electrospinning, acetic acid is a GRAS solvent and can dissolve both the polymers and the selected AIs.

In more detail, CNCs (3.5%, w/w content, 140 nm long and 20 nm in diameter) were synthesized as previously described.[29] After vortexing for 10 s, 1 mL of suspension was mixed into 4 mL of acetic acid in a vial and the solution was stirred for another 20 min. Subsequently, zein (zein from maize, Sigma-Aldrich, Z3625) and starch (Ingredion, Hylon V, corn starch, 55% amylose content) were added at an 85:15 (w/w) ratio (zein:starch) into the solution. Pristine fibers were synthesized using electrospinning by loading the solutions in a 10 mL plastic syringe (BD Luer-Lock tip) and were supplied by a syringe pump through a stainless steel single-needle injector (diameter: 0.6 mm, 90° blunt end) toward the collector. High voltage was applied to both the needle injector tip and collector from the power supply. The electrospinning process parameters such as flow rate, needle-collector distance, total polymer concentrations, and applied voltage were modified to obtain bead-free fibers. The environmental parameters such as temperature and RH were 25 °C and 30% RH, respectively, whereas the final operational electrospinning parameters are summarized in Table S1. The fibers were randomly deposited on aluminum foil (20 × 20 $cm^2$). The mass of the fibers per surface area was adjusted to 2.5 mg/$cm^2$ (or 1.25 mg/$cm^2$) by adjusting electrospinning time.

*Synthesis of Multistimuli-Responsive Fibers.* Since the goal was to produce both enzyme and RH response functionalities to the fibers, we incorporated a cocktail of both free AIs and CD-ICs of AIs. The cocktail comprised the nature-derived free AI thyme oil, citric acid, and nisin, as described in our previous study.[9] Separately, CD-ICs of thyme oil, sorbic acid, and nisin were synthesized and incorporated into fibers to provide RH response due to the unique structure of CDs.

These multistimuli-responsive fibers were synthesized by incorporating both the cocktail of free AIs and CD-ICs of AIs into the solution of CNCs, zein, and starch by direct solution integration.[9] First, a cocktail of AIs (1%, w/v, thyme oil; 5%, w/v, citric acid (VWR, citric acid 10% w/v aqueous solution); 0.2% w/v, nisin) was dissolved in 4 mL of acetic acid. The composition of the AI cocktail and its optimization in terms of food-related antimicrobial efficacy was determined in our previous study.[9] One milliliter of CNC (3.5% w/w) solution was vortexed for 10 s and then mixed into this solution, followed by stirring for 20 min. Then, γ-CD/thyme oil-IC (1:2), γ-CD/sorbic acid-IC (1:2), and 0.023 g γ-CD/nisin-IC (4:1) corresponding to 1% (w/v) thyme oil, 0.5% (w/v) sorbic acid, and 0.2% (w/v) nisin were added into the solution while stirring. Finally, 2.56 g of zein and 0.43 g of starch (85:15) were added into the solution, and after a complete dissolution of all components, electrospinning was performed. The solution was loaded into a 10 mL plastic syringe (BD Luer-Lock tip), and process parameters including flow rate, needle-collector distance, and applied voltage were adjusted to yield bead-free multistimuli-responsive fibers that were randomly deposited on aluminum foil by electrospinning. The environmental parameters such as temperature and RH were 25 °C and 30% RH, respectively, whereas the final operational parameters are presented in Table S1. Fibers with free AI cocktails only or with CD-ICs of AIs only were also synthesized as control samples and were denoted as enzyme-responsive fibers or RH-responsive fibers, respectively. Two separate mass per surface area fibers were synthesized by varying the deposition times: 1.25 and 2.50 mg/$cm^2$.

**Morphological/Size Characterization of Fibers.** Morphological characterization of the fibers was performed by scanning electron microscopy (SEM, Zeiss FESEM Ultra Plus). Prior to imaging, the fiber samples were cut into small pieces and mounted on a stub using double-sided carbon tape. The average diameter of the fibers was calculated using ImageJ Software ($n$ = 100), and the results are given as average ± standard deviation. The specific surface area ($m^2$/g), average pore radius (nm), and total pore volume ($cm^3$/g) of the fibers were measured by a Brunauer−Emmett−Teller (BET, Quantachrome NOVA touch LX4) surface area analyzer. Prior to BET measurement, fiber samples in a 9 mm cell were degassed at 313.15 K for 12 h. Finally, low-temperature (77.35 K) nitrogen adsorption isotherms were measured at relative pressures from 0.005 to 1.00.

**Chemical and Crystallinity Characterization of Fibers.** The crystallinity of the fibers was investigated by XRD (Bruker D2 Phaser) in the 2θ range of 5−40° using Cu Kα radiation. The chemical characterization of fibers was investigated using ATR-FTIR (Thermo Scientific Nicolet IS50), and the spectra were recorded between 4000 and 400 $cm^{-1}$ at a resolution of 4 $cm^{-1}$, and 64 scans/sample were taken.

**AI Release Kinetics.** *Determination of AI Content in the Fibers.* The AI content of fibers was determined by dissolving 15 mg of fiber samples in 10 mL of ethanol. The solutions were then filtered using cellulose acetate filter (0.45 μm), and analysis was performed by liquid chromatography with high-resolution mass spectrometry (LC/HRMS), as described below. The AI concentration is calculated and compared to the theoretical values from the concentrations in solution used during electrospinning and is then used in the calculation of the released thymol in the enzyme and multistimuli-responsive fibers.

*Liquid Chromatography with High-Resolution Mass Spectrometry (LC/HRMS) Analysis.* The AI release kinetics under various stimuli were quantified in controlled dissolution experiments. It is worth noting that for the release kinetics studies, thyme oil release was measured as a representation of the release behavior under various


https://doi.org/10.1021/acsami.1c12319
ACS Appl. Mater. Interfaces 2021, 13, 50298−50308

stimuli conditions. The release of other AIs under stimuli conditions may not be the same as that of thyme oil. Thymol, the major compound of thyme oil (60%), was selected as a surrogate of AI quantitation for chemical analysis by LC/HRMS (Dionex Ultimate 3000 Liquid Chromatograph interfaced to a Thermo Q-Exactive HRMS). The LC was run on an Agilent SB-C18 2.1 × 150 column at 0.2 mL/min. Mobile phase A was water with 1% formic acid, and mobile phase B was acetonitrile with 1% formic acid. After a 1 min hold at 50% B, there was a linear gradient for 9 min to 95% B, where it was held for 3 min followed by a 3 min re-equilibration at 50% B. The MS was operated using positive electrospray at 3.5 kV, with the capillary and auxiliary gas temperatures set to 300 °C, and the gas flows were as follows: sheath 50, auxiliary 15, and sweep 10. For quantitation of thymol, we isolated a 3 $m/z$ window around the $(M + H)^+$ ion, fragmented it at a collision energy of 20, collected a full scan of the fragments between $m/z$ = 50 and 175 at a resolution of 17 500, and monitored the sum of the $m/z$ = 91.0547 and 109.09656 fragments. The area of each peak was converted to concentration (ppm) using standard calibration curves. The release experiments were carried out in triplicate, and the results were reported as average ± standard deviation. More details are given in the next section.

*Bacterial Enzyme-Triggered AI Release Kinetics from Fibers.* Enzyme-responsive fibers that were incorporated with only free AIs (no CD-ICs) were placed in enzyme solutions in phosphate-buffered saline (PBS, VWR, pH:7.4) at 0.1, 1, and 3 U/mL concentrations for 12 h. Enzyme solutions prepared in PBS consisted of protease (Sigma-Aldrich, P5147, protease from Streptomyces griceus), α-amylase (Sigma-Aldrich, 10065, amylase from Aspergillus oryzae), and cellulase (Sigma-Aldrich, C1184, cellulase from Aspergillus niger) at a 1:1:1 ratio. Fibers were immersed in enzyme solutions in an incubator at 37 °C and shaken for 12 h. It is worth mentioning that the 37 °C temperature was not selected as a proxy for food storage conditions but because this temperature is the optimum temperature for enzymatic activity for all of the three enzymes selected. After incubation, the morphology of the fibers was observed by SEM (Zeiss FESEM Ultra Plus). Separately, 15 mg of enzyme-responsive fibers was immersed in 10 mL of 1 U/mL enzyme solution (protease:amylase:cellulase, 1:1:1). The samples were kept in an incubator at 37 °C for 12 h. As a control, enzyme-responsive fibers were also immersed in 10 mL of PBS without enzymes. A 1 mL of aliquot sample was withdrawn at 1, 4, and 12 h and was replaced with the same volume of either enzyme or PBS solution. The solutions were passed through a cellulose acetate filter (0.45 μm) and were analyzed by LC/HRMS, as described above. The measured concentration of thymol in the fibers was used to convert the concentration of the released thymol into percent values.

*RH-Triggered AI Release Kinetics from Fibers.* Fifteen milligrams of RH-responsive fibers incorporated with only CD-ICs of AIs (no free AIs) were placed into two environmental chambers with 50% and 95% RH values. The RHs in the chambers were controlled using saturated solutions of $Mg(NO_3)_2$ and $KNO_3$ (VWR Chemicals, BDH Prolabo, Australia). The temperature in the two chambers was constant at room temperature. At three time points including 1, 2, and 4 h, samples were taken out of the chamber and placed in 10 mL of ethanol to extract the thymol left in the fibers. The solutions were then filtered through cellulose acetate filter (0.45 μm) and analyzed by LC/HRMS. The release experiments were carried out in triplicate, and the results are summarized as the remaining concentration of thymol (ppm) in the fibers for the two RH conditions. Additionally, SEM (Zeiss FESEM Ultra Plus) images were also taken after fiber removal from the chambers to observe any changes in their morphology as a function of RH.

*AI Release Kinetics from Fibers into Water.* The release kinetics experiments were also performed by immersing the multistimuli-responsive fibers (15 mg) in 10 mL of water to simulate an aqueous-based food environment. A 1 mL of aliquot samples was withdrawn at 6, 12, and 24 h and was then replaced with the same volume of water. The sample solutions were then filtered using cellulose acetate filter (0.45 μm) and analyzed by LC/HRMS.

**Assessment of Antimicrobial Efficacy of Multistimuli-Responsive Fibers.** *Strain Information.* *Escherichia coli* ATCC 25922 (*E. coli*), *Listeria innocua* ATCC 33090 (*L. innocua*), and *Aspergillus fumigatus* ATCC 96918 (*A. fumigatus*) were used in this study as representative Gram-negative, Gram-positive, and fungal food pathogens, respectively. *E. coli* ATCC 25922 has been regarded as a nonpathogenic surrogate organism for the pathogenic *E. coli* O157:H7 and *L. innocua* surrogate for the pathogenic *L. monocytogenes*. *A. fumigatus* is a widely spread fungus, which causes food spoilage, as well as produces mycotoxins that cause human illness.[30] *E. coli* and *L. innocua* were resuscitated and streak-plated from stock solutions and maintained on tryptic soy agar (TSA; Hardy Diagnostic, Santa Maria, CA) at 4 °C. A single colony from TSA was transferred into 10 mL of tryptic soy broth (TSB; Hardy Diagnostic, Santa Maria, CA). After incubation at 37 °C for 24 h, the bacterial broth was centrifuged at 3000 rpm for 15 min (Allegra 6R, Beckman Coulter, Indianapolis, IN). After discarding the supernatant, 2 mL sterile 0.1% (w/v) peptone water was used to resuspend the bacterial pellet. The cell density was adjusted to ~$10^8$ colony forming unit (CFU)/mL with peptone water with a final optical density (O.D.) 600 value to 0.2. The freeze-dried *A. fumigatus* was rehydrated in sterile deionized water and further translated onto a malt extract agar (MEA) and incubated at 30 °C for 3 days. To produce mature conidia, a single colony was further incubated on MEA at 30 °C for 7 days until the colony became dark green. Mature spores were harvested from the lawn and then diluted with deionized water. The final concentration of spores was adjusted to ~$10^7$ CFU/mL using a manual hemocytometer (Diagnocine, Hackensack, NJ).

*Direct Contact Assay.* The direct contact assay to assess the antimicrobial efficacy test of fibers was conducted as described previously by the authors (Figure S1a).[9] Briefly, 100 μL of the microbial culture concentration was diluted in 10 mL of agar slurry (0.85% NaCl, 0.3% agar). Three hundred microliters of the inoculated agar slurry was then inoculated onto a 2 × 2 $cm^2$ fibers deposited in aluminum foil and then placed into a 6-well plate (Thermo Scientific, 145380). After 5 min of contact time, the agar slurry formed a gel layer on top of the fibers with a thickness of less than 1 mm. The plates were then transferred into an incubator at 37 °C for 1 and 24 h. To avoid drying out of the gel during exposure, a reservoir full of water was used to maintain the RH at approximately 70%.

*Enumeration.* After 1 and 24 h, each test sample was transferred into a sterile Whirl-Pak bag with 2.7 mL of PBS to reach a first 10-fold dilution. The sample bag was homogenized with a stomacher for 2 min at a normal speed. The homogenate and its serial dilutions were poured-plated and incubated. Specifically, *E. coli* and *L. innocua*were cultured on TSA 100 μL of proper dilution and incubated at 37 °C for 24 h, whereas for *A. fumigatus* 100 μL of dilution was grown on MEA and incubated at 30 °C for 48 h.

**Relative Humidity-Triggered Antimicrobial Efficacy of Fibers.** *E. coli* was used as a model organism to validate the antimicrobial efficacy of RH-responsive fibers at high RH conditions. Dry inoculation method was used to avoid the introduction of extra moisture into the chambers. The detailed experimental steps are illustrated in Figure S1b. Ten microliters of bacterial culture (~$10^8$ CFU/mL) was applied by 10 1 μL aliquots on an aluminum foil substrate to reach a final inoculation level of $10^6$ CFU/sample. The inoculated aluminum foil was further dried in a biosafety cabinet for 10 min. RH-responsive fibers (2.50 mg/$cm^2$) were placed on top of the aluminum foil and covered with the dried bacterial cells, and a binder clip was used to let the fibers and bacterial cells contact tightly. The two-layer system was transported into two RH-controlled environmental chambers, which maintained 50% and 95% RH conditions. Both chambers were maintained at room temperature (22 °C). The two-layer samples were kept in the environmental chambers for 15 min and 1 h. Afterward, the aluminum foil with bacteria was decoupled from the fibers and transported into a centrifuge tube with 1 mL of peptone water. The tube was then vortexed sufficiently for at least 2 min to make sure the bacteria were detached from the aluminum foil. Serial dilution was performed and followed by plating on TSA and incubation at 37 °C for 24 h. To


https://doi.org/10.1021/acsami.1c12319
ACS Appl. Mater. Interfaces 2021, 13, 50298−50308

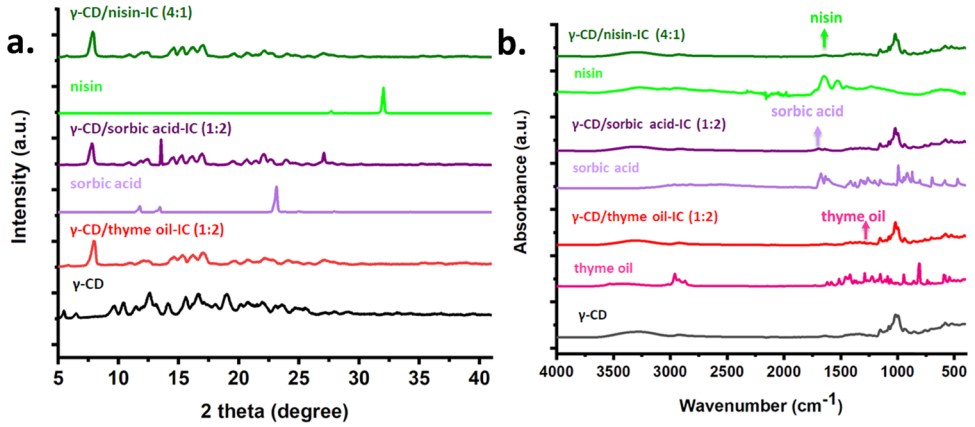


**Figure 3.** (a) X-ray diffraction (XRD) patterns of γ-CD, active ingredients (AIs), and cyclodextrin-inclusion complexes (CD-ICs) of AIs; (b) attenuated total reflectance-Fourier transform infrared (ATR-FTIR) spectrometry spectra of γ-CD, AIs, and CD-IC of AIs.

detect if there were any bacterial cells left on the fibers, the fibers detached from the bacterial-inoculated aluminum foil were transported into a centrifuge tube with 1 mL of peptone, and 100 μL of solution was poured-plated on TSA for enumeration at 37 °C for 24 h. As a control, the inoculated aluminum foil without fibers and attached with the pristine fibers were also used at 50% RH and 95% RH conditions followed by the same protocol described above for the *E. coli* enumeration.

*Statistical Analysis.* Three independent replicates were conducted for each condition. The number counts of each microorganism were converted into log CFU/sample. One-way ANOVA within the confidence interval of 95% ($P < 0.05$) was performed for significant analysis (IBM SPSS Statistics for Windows, version 19.0, IBM Corp., Armonk, NY). Statistical analysis to illustrate the difference within the same fibers (uppercase letter) and within the same contact time (lowercase letter) was performed. LSD and Tukey's post hoc tests were used to avoid type 1 error while retaining the statistical power (IBM SPSS Statistics for Windows, version 19.0, IBM Corp., Armonk, NY). Significant difference within the same fibers was labeled with uppercase letters ("A" or "B" was used for 50% RH, "C" or "D" were used for 95% RH). Significant difference within the same contact time was labeled with lowercase letters ("a" or "b" was used for 50% RH, "c" or "d" was used for 95% RH). To illustrate the difference of RH-responsive fibers against *E. coli* at different RH levels, significant difference among data in the same contact time was labeled with * (***$P \leq 0.001$, *$P \leq 0.05$).

## RESULTS AND DISCUSSION

**Physicochemical Characterization of CD-ICs.** XRD analysis was used to characterize the crystallinity of γ-CD, γ-CD/thyme oil-IC (1:2), sorbic acid, γ-CD/sorbic acid-IC (1:2), nisin, and γ-CD/nisin-IC (4:1) and more importantly to confirm the formation of CD-ICs (Figure 3a). Sorbic acid has its characteristic 2θ peaks at 11.8, 13.4, and 23.2°, whereas nisin has its characteristic peak at 2θ 32.0°. The absence of the characteristic of sorbic acid and nisin peaks in γ-CD/sorbic acid-IC (1:2) and γ-CD/nisin-IC (4:1) indicates successful CD-IC formation. Furthermore, the major cage-type crystalline characteristic peaks of γ-CD are observed at 2θ 5.5, 6.5, 9.6, 10.4, 11.5, 12.6, 14.1, 15.6, 16.7, and 19.0°. Pristine CDs have cage-type crystalline structures, but when CD-ICs are formed, a channel-type crystalline structure is formed with characteristic peaks.[28] In the CD-ICs, characteristic channel-type peaks of γ-CD-IC were observed at 2θ 7.8, 14−17, and 22° for γ-CD/thyme oil-IC, γ-CD/sorbic acid-IC, and γ-CD/nisin-IC, respectively. Collectively, these findings confirm that CD-ICs of thyme oil, sorbic acid, and nisin were successfully synthesized.

Figure 3b shows the ATR-FTIR spectra of the CD-ICs and further confirms CD-IC synthesis. First, the peak at 1696 $cm^{-1}$ confirms the presence of the C═O stretching of sorbic acid[31] in the sorbic acid−CD-IC. Second, the intensity increments of the peak at 1250 $cm^{-1}$ correspond to the C−O stretching of thyme oil in the spectra of the thyme oil−CD-IC[32] and the peak at 1643 $cm^{-1}$ in the spectra of nisin−CD-IC[33] confirms the presence of thyme oil[32] and nisin. Third, the characteristic peaks of CDs were evident at 3000−3630 $cm^{-1}$ (OH stretching), 2929 $cm^{-1}$ (C−H stretching), 1643 $cm^{-1}$ (H-OH bending), 1150 $cm^{-1}$ (C−O−C glycosidic antisymmetric stretching), 1078 $cm^{-1}$ (C−O stretching), and 1020 $cm^{-1}$ (C−C stretching). It is worth noting that the CD-associated peaks shifted from 3281 to 3310 and 1150 to 1154 $cm^{-1}$ for thyme oil−CD-IC, 1018 to 1022 $cm^{-1}$ for sorbic acid−CD-IC, and 1018 to 1021 $cm^{-1}$ for nisin−CD-IC. These peak shifts observed in each CD-IC highlight the interactions between CD and the guest molecules and further confirm successful CD-IC formation.[34]

**"Green" Synthesis of Stimuli-Responsive Fibers.** Table S1 summarizes the AI concentrations (%), polymer compositions (%), and other electrospinning operational parameters used for the synthesis of multistimuli-responsive fibers, as well as for the control pristine fibers (no AIs), enzyme-responsive fibers (no CD-ICs, only free AIs), and RH-responsive fibers (no free AIs, only CD-ICs). Here, polymers such as zein, starch, and cellulose were selected by design to form the backbone of the fibers. The fibers were loaded with AIs, and as the polymers are degraded by specific enzymes secreted from microorganisms, they will accelerate the release of AIs. Furthermore, the fibers will also be loaded with CD-ICs of AIs to make them RH-responsive. The unique inherent structure of CD-ICs will enable the release of AIs when the RH is above 85%. As a result, the developed fibers will be responsive to both enzymes and RH. Such multistimuli-responsive fibers are ideal to be used to endow antimicrobial properties to food packaging materials. The use of CD-ICs as an RH-responsive release system rather than improving the solubility of hydrophobic compounds for drug delivery applications[35] is also highly novel.

**Morphological Characterization of Fibers.** SEM images of pristine, enzyme-responsive, RH-responsive, and multi-stimuli-responsive fibers are shown in Figure 4a−d, along with


https://doi.org/10.1021/acsami.1c12319
ACS Appl. Mater. Interfaces 2021, 13, 50298−50308

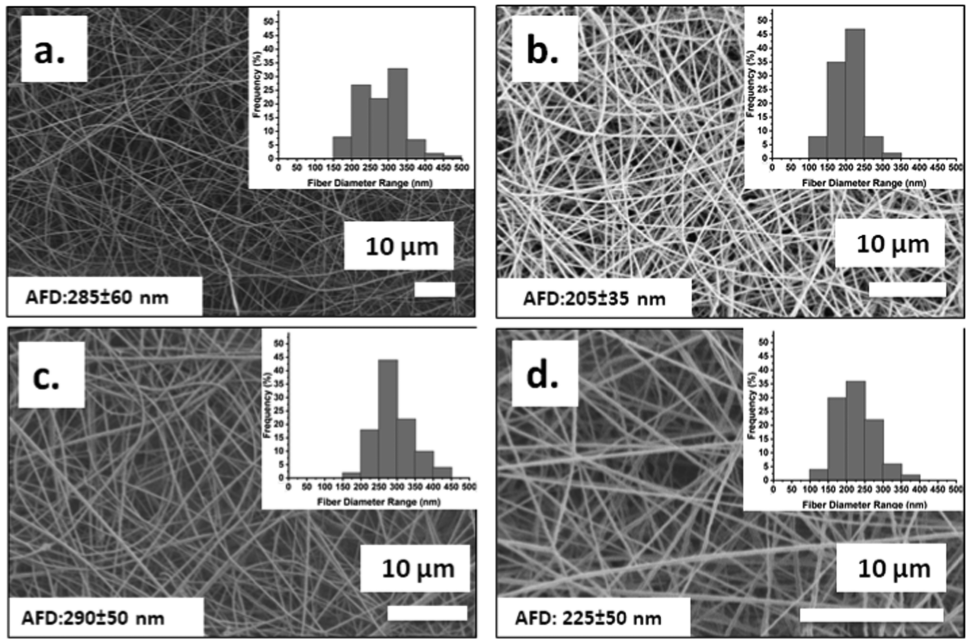


**Figure 4.** Scanning electron microscopy (SEM) images with the average fiber diameter (AFD) distribution of (a) pristine fibers, (b) enzyme-responsive fibers with only free active ingredients (AIs), (c) relative humidity (RH)-responsive fibers with only cyclodextrin-inclusion complexes (CD-ICs) of AIs, and (d) multistimuli-responsive fibers.

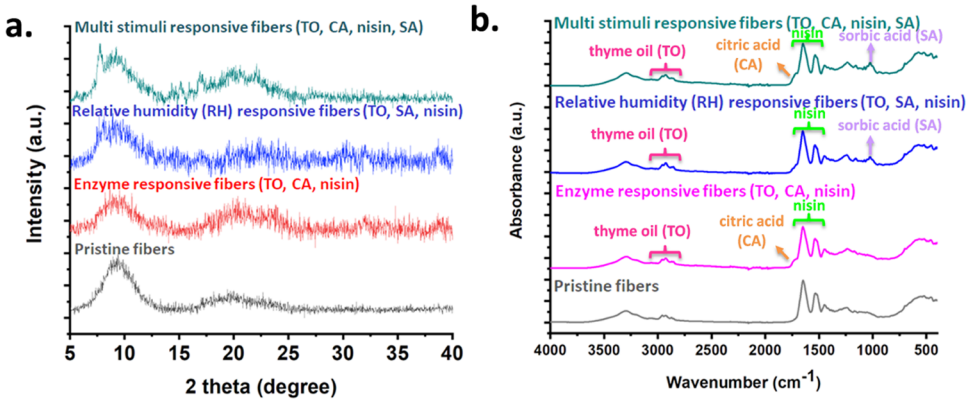


**Figure 5.** (a) X-ray diffraction (XRD) patterns and (b) attenuated total reflectance-Fourier transform infrared (ATR-FTIR) spectrometry spectra of pristine fibers; enzyme-responsive fibers with only free active ingredients (AIs): thyme oil (TO), citric acid (CA), and nisin; relative humidity (RH)-responsive fibers with only cyclodextrin-inclusion complexes (CD-ICs) of AIs: TO, sorbic acid (SA), and nisin; and multistimuli-responsive fibers with both free AIs (TO, CA, nisin) and CD-IC of AIs (TO, SA, nisin).

the average fiber diameters (AFDs) and diameter distribution graphs. All fibers exhibited bead-free and uniform morphology by SEM. The AFDs of pristine, enzyme-responsive, RH-responsive, and multistimuli-responsive fibers were calculated from SEM images as 285 ± 60, 205 ± 35, 290 ± 50, and 225 ± 50 nm, respectively. It is worth noting that emphasis was given to produce various types of fibers with AFDs in the range of 200−300 nm by adjusting the operational electrospinning parameters. Fiber diameter distributions ranged from 100 to 500, 100 to 350, 150 to 450, and 100 to 450 nm for the pristine, enzyme-responsive, RH-responsive, and multistimuli-responsive fibers, respectively.

**Physicochemical Characterization of the Fibers.** Table S2 summarizes the specific surface area (SSA, $m^2/g$), average pore radius (nm), and total pore volume ($cm^3/g$) of the various fibers. The multipoint BET surface areas of pristine, enzyme-responsive, RH-responsive, and multistimuli-responsive fibers were 12.1, 19.3, 10.4, and 10.9 $m^2/g$, respectively. The SSAs of the enzyme-responsive fibers are greater than those of the others due to the lower AFD (205 nm), whereas the SSAs of other fibers are all quite similar. The slight changes in AFDs resulted in the SSA differences in the fibers. The average pore radii for pristine, enzyme-responsive, RH-responsive, and multistimuli-responsive fibers were 2.18, 1.64, 1.56, and 2.16 nm, respectively. Finally, the total pore volumes were $1.32 \times 10^{-2}$, $1.58 \times 10^{-2}$, $0.81 \times 10^{-2}$, and $1.18 \times 10^{-2}$ $cm^3/g$ for pristine, enzyme-responsive, RH-responsive, and multistimuli-responsive fibers, respectively. These total pore volume values are consistent with the literature as pore volume tends to increase with the SSA.[36] High SSA of fibers will enable miniscule quantity of fibers and antimicrobials due to the high surface-to-volume ratio and optimize antimicrobial efficacy while minimizing potential sensory effects from the antimicrobials used.

Figure 5a shows the crystallinity of pristine, enzyme-responsive, RH-responsive, and multistimuli-responsive fibers


https://doi.org/10.1021/acsami.1c12319
ACS Appl. Mater. Interfaces 2021, 13, 50298−50308

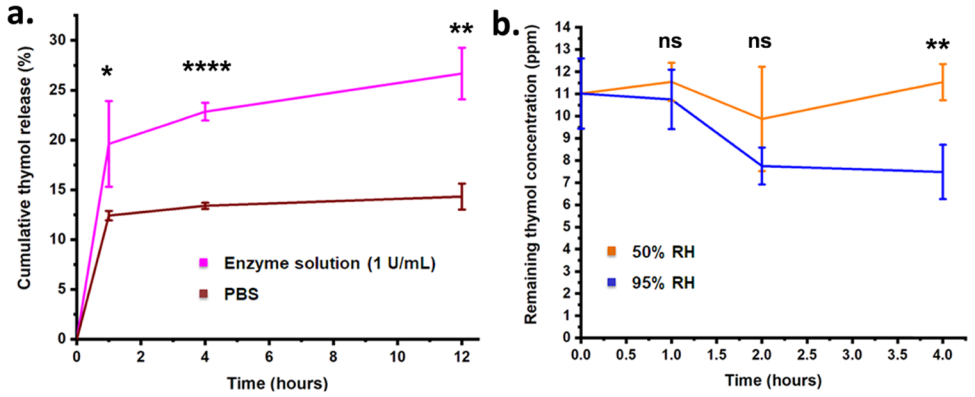


**Figure 6.** (a) Cumulative release (%) of thymol from enzyme-responsive fibers with only free active ingredients (AIs) into enzyme solution and PBS without enzymes, (b) remaining thymol concentration (ppm) from relative humidity (RH)-responsive fibers with only cyclodextrin-inclusion complexes (CD-ICs) of AIs at 50% RH and 95% RH as a function of time. The error bars in the figure represent the standard deviation (SD). The significant difference among data in the same contact time was labeled with nonsignificant (ns): $P > 0.05$, * $P \leq 0.05$, ** $P \leq 0.01$, or **** $P \leq 0.0001$.

using XRD. All fibers exhibited broad amorphous peaks for zein and starch at $2\theta$ 5−12.5 and 16.5−25.0°, respectively. In electrospinning, crystalline formation for small molecules is significantly hindered due to the rapid solvent evaporation during the process.[37] This is the case for the enzyme-responsive fibers, where the crystalline peak of nisin at $2\theta$ 30° was not evident. However, this may also be related to the miniscule quantity of nisin and the dominance of the amorphous polymers in the fibers. In addition, RH-responsive and multistimuli-responsive fibers show peaks at $2\theta$ 7.8 and 14−17°, respectively, indicative of the channel-type crystalline nature due to the formation of CD-ICs. However, these peaks are more prominent in the case of multistimuli-responsive fibers due to the lower concentration of polymers (41% w/v) present related to the enzyme-responsive fibers (47% w/v). In summary, the XRD patterns reveal the successful incorporation of CD-ICs in the electrospun fibers and align well with the literature for $\gamma$-CD-ICs.[38]

The chemical composition of the pristine, enzyme-responsive, RH-responsive, and multistimuli-responsive fibers was investigated by ATR-FTIR (Figure 5b). Thyme oil has peaks at 2960−2850 $cm^{-1}$ belonging to the C−H stretching vibration of $CH_3$.[32] The enzyme-responsive, RH-responsive, and multistimuli-responsive fibers exhibited this broad peak, which confirms the presence of thyme oil in the fibers. Nisin has two peaks at 1650 and 1522 $cm^{-1}$, which are attributed to the amide I and II bonds in the structure.[33] These peaks are also evident in the enzyme-responsive, RH-responsive, and multistimuli-responsive fibers, confirming the presence of nisin in the fibers. It is also worth noting that these same peaks in the spectra of pristine fibers are attributed to zein, which also has amide I and II bonds in its structure. Finally, the C═O stretching band of citric acid[39] is observed at the spectra in 1721 $cm^{-1}$, and as expected, this peak was only observed in enzyme-responsive and multistimuli-responsive fibers. The trans alkene peaks of sorbic acid are observed at 1000 $cm^{-1}$ in the RH-responsive and multistimuli-responsive fibers, which have sorbic acid in the CD-IC.[31] In summary, the FTIR spectra further confirm the successful incorporation of all AIs in the various fibers.

**Triggered Release Kinetics of Antimicrobial AIs.** *Bacterial Enzyme-Triggered AI Release.* For the enzymatic release kinetic studies, to enhance chemical analytical sensitivity from the miniscule amounts of AIs released, CD-ICs were excluded in the synthesis of the fibers and only free AIs were used. The cumulative release (%) of thymol from enzyme-responsive fibers as a function of time is shown in Figure 6a. The concentration of thymol in the fibers was found to be at 96% of the expected theoretical calculation, demonstrating highly efficient loading. The release of thymol reached a plateau at 4 h and remained relatively constant at 13 and 23% for PBS and enzymatic conditions, respectively. Importantly, a significantly higher quantity of thymol was released in the presence of enzymes as compared to that of PBS, highlighting the responsiveness of the fibers and demonstrating the different mechanisms involved in cargo. In PBS, the fibers released thymol by diffusion, but in the enzyme solution, the thymol is released both by diffusion and by biopolymer degradation by enzymes. Of interest is Figure S2a−c, which shows the enzymatic degradation of the fibers at 0.1, 1, and 3 U/mL. The degradation of fibers at 1 U/mL increases significantly as compared to the low level of enzyme (0.1 U/mL), in which degradation was minimal. However, when the concentration further increases to 3 U/mL, complete degradation of fibers is observed. Therefore, 1 U/mL was chosen to confirm the enzymatic release of AIs from the fibers.

*Relative Humidity (RH)-Triggered AI Release.* For the release kinetic studies under different RH conditions, free AIs were excluded from the synthesis of the fibers for the case of RH-triggered release and only CD-ICs were used to enhance chemical analytical sensitivity from the miniscule amounts of AIs released. The concentration of thymol in the RH-responsive fibers was found to be at 91% of the expected theoretical calculation. The remaining concentration of thymol in RH-responsive fibers at 50% and 95% RH levels is shown in Figure 6b. The thymol concentration reached a plateau at ∼7.5 ppm after 4 h for the 95% RH condition, significantly lower than the ∼11.5 ppm level for the 50% RH condition. This confirms that the fibers behave as designed, releasing more thymol at higher humidity. It is worth mentioning that there are published studies showing that CD-ICs with volatile compounds such as limonene showed minimum evaporation for 50 days at 18% RH and room temperature. At 100 days, only 25% of limonene was lost.[40] CD-ICs release a significant quantity of antimicrobials when the RH exceeds a certain limit (85%). If the RH does not reach 85%, AIs will remain intact in


https://doi.org/10.1021/acsami.1c12319
ACS Appl. Mater. Interfaces 2021, 13, 50298−50308

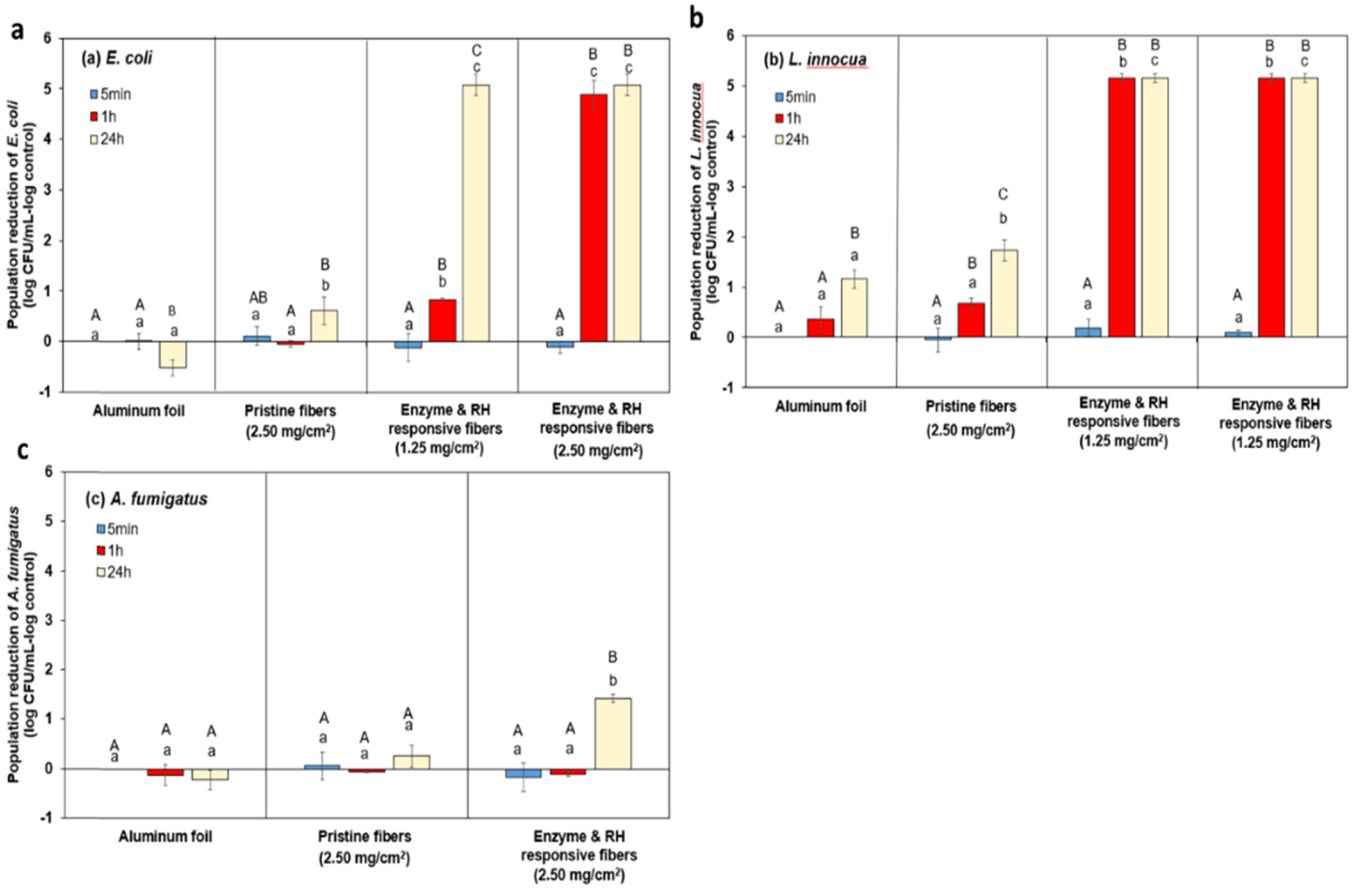


**Figure 7.** Antimicrobial activity of multiresponsive fiber against (a) *E. coli*, (b) *L. innocua*, and (c) *A. fumigatus*. Aluminum foil and pristine fibers were used as controls. 2.50 and 1.25 mg/cm$^2$ represent the mass per surface area of fibers. Data in the same material labeled with different uppercase letters is significantly different ($P < 0.05$). Data in the same treatment time group labeled with different lowercase letters is significantly different ($P < 0.05$).

the fibers. Therefore, CD-IC stability is quite good in the air at room conditions. In addition, SEM images (Figure S3a,b) also demonstrate that RH-responsive fibers are intact and not wetted at the end of the 4 h at 50% RH, whereas the fibers at 95% RH maintain their fibrous morphology but are swollen and merged. Statistical analysis between the groups in each responsive release experiment was performed using the unpaired *t*-test (independent variants).

*AI Release Kinetics from Fibers in Aqueous Food Simulant (Water).* The initial AI concentration of fibers was determined to be 89% and was used to calculate the percentage of thymol released. The cumulative release (%) of thymol from the multistimuli-responsive fibers into water, a nonacidic aqueous food simulant, as a function of time is shown in Figure S4. There is a rapid AI release in 6 h (21%), and then a plateau is reached. This is attributed to the high specific surface area of fibers as shown by BET, as well as the wettability of the fibers owing to the nature of polymers used in the synthesis. The slight decrease (~4%) in the release of thymol from 12 h (21.4 ± 1.8%) to 24 h (17.3 ± 2.5%) is most likely due to the interference of the degraded polymers, which makes it difficult to precisely calculate the thymol peaks.

**Antimicrobial Efficacy of Multistimuli-Responsive Fibers.** Figure 7a–c summarizes the antimicrobial efficacy of multistimuli-responsive fibers against *E. coli*, *L. innocua*, and *A. fumigatus*. Aluminum foil and pristine fibers were included as controls. Two levels of fiber mass per surface area were tested: 2.5 and 1.25 mg/cm$^2$. More details are given in the next section.

*E. coli and L. innocua.* In general, aluminum foil and pristine fibers (controls) did not support or inhibit the growth of *E. coli*; the population fluctuation within 24 h was less than 1 log. The responsive fibers reduced *E. coli* and *L. innocua* growth by 5 logs (under the detection limit) at 1 and 24 h contact time, respectively. Notably, when the mass per surface area of multistimuli-responsive fibers decreased from 2.50 to 1.25 mg/cm$^2$, the antimicrobial efficacy against *E. coli* reduced from ~5 log to ~1 log at a contact time of 1 h. However, for *L. innocua*, the treatment with a lower mass per surface area did not show reduced antimicrobial efficacy at both 1 and 24 h and exhibited 5 logs reduction for both contact times. Similar fiber mass per surface dependency was found in our previous publication using antimicrobial zein fibers.[9]

In summary, the multistimuli-responsive fibers developed in this study showed an excellent inactivation efficacy against both Gram-negative bacteria and Gram-positive bacteria with 24 h contact time. The antimicrobial activity of multistimuli-responsive fibers seems to be fiber mass per surface area- and time-dependent for *E. coli* but not *L. innocua* although that is dependent on the species of bacteria. However, 24 h contact time is sufficient to release enough AIs for bacterial inactivation. In addition, these results are also in consistent with the results reported in the literature for the nature-derived antimicrobials used in this study.[8,41−44]


https://doi.org/10.1021/acsami.1c12319
ACS Appl. Mater. Interfaces 2021, 13, 50298−50308

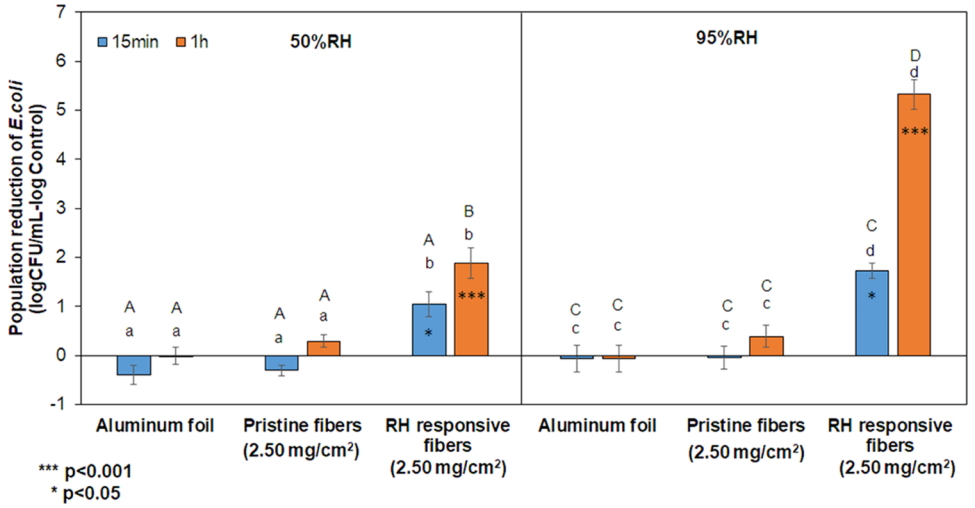


**Figure 8.** Antimicrobial activity of relative humidity (RH)-responsive fibers (2.50 mg/cm$^2$) against *E. coli* at 50% RH and 90% RH. At the same RH level, data in the same material labeled with different uppercase letters is significantly different ($P < 0.05$). Data in the same contact time labeled with different lowercase letters is significantly different ($P < 0.05$). At different RH levels, significant difference among data in the same contact time of RH-responsive fibers was labeled with *: *** $P \leq 0.001$, * $P \leq 0.05$. The error bars in the figure represent the standard deviation (SD).

*Antifungal Efficacy.* The antifungal efficacy of the multistimuli-responsive fibers was also assessed for the 2.50 mg/cm$^2$ mass loading. Aluminum foil and pristine fibers were used as controls and had minimal influence on the fungal growth (with less than 0.2 log population change after 24 h contact time). As shown in Figure 7c, a significant population reduction (1.4 log) of *A. fumigatus* was evident after 24 h contact time. The antifungal efficacy of the multistimuli-responsive fibers may be attributed to the presence of thyme oil in the AI cocktail since thymol has proven antifungal efficacy.[45] Previous studies have reported thymol to have a minimum inhibitory concentration (MIC) of 150−190 $\mu$g/mL and a minimum fungicidal concentration (MFC) of 175−384 $\mu$g/mL against *A. fumigatus*.[46,47]

**Relative Humidity (RH)-Triggered Antimicrobial Activity.** The antimicrobial efficacy of responsive fibers at 50% and 95% RH conditions is shown in Figure 8. In general, aluminum foil and pristine fibers (controls) did not support or inhibit the growth of *E. coli* at both RH) conditions. With 1 h contact time, RH-responsive fibers were able to achieve 5 log reductions (under the detection limit) of *E. coli* at 95% RH, while only 1.9 log reduction at 50% RH indicative of their ability to trigger AI release at high RH levels. It is worth noting that based on the statistical analysis, there was a significant ($P < 0.05$) difference in the population reduction of *E. coli* between 50% RH and 95% RH conditions at both contact times (15 min and 1 h) (labeled with *). At the same RH level, the population reduction of *E. coli* increased significantly ($P < 0.05$) with the increase of contact time, indicating that the antimicrobial agents incorporated in RH-responsive fibers released in a time-dependent manner.

To summarize, the biodegradable, nontoxic, multiresponsive biopolymer-based antimicrobial fibers developed in this study are ideal for use in active food packaging applications. The synthesis of CD-ICs from nature-derived and FDA GRAS-approved antimicrobials is highly novel, and to the best of our knowledge, this is the first time CD-ICs were used in responsive food packaging beyond their extensive use in drug delivery[35] and recent few studies in food packaging.[8]

## CONCLUSIONS

Developing responsive release systems is of great importance in addition to the sustainable and biodegradable active food packaging to the food industry due to the significant negative environmental impact of petroleum-based polymers that are currently widely used. Here, biopolymer-based, biodegradable, and enzyme- and relative humidity (RH)-responsive antimicrobial fibers were developed using electrospun cellulose nanocrystals (CNCs), zein (protein), and starch and a cocktail of both free nature-derived antimicrobials including thyme oil, citric acid, and nisin and also cyclodextrin-inclusion complexes (CD-ICs) of thyme oil, sorbic acid, and nisin. The fibers were designed to release their free AIs and CD-ICs of AIs in response to enzyme and RH triggers, bringing precision in the AI delivery while achieving superior antimicrobial functionality for a broad range of food-related pathogenic bacterial and spoilage microorganisms. The use of FDA GRAS-approved materials and green synthesis processes makes these nontoxic, biodegradable multistimuli-responsive fibers ideal for sustainable food packaging materials.

## ASSOCIATED CONTENT

### Supporting Information

The Supporting Information is available free of charge at https://pubs.acs.org/doi/10.1021/acsami.1c12319.

The composition of fibers and operational parameters applied to produce fibers (Table S1); surface area analysis of fibers (Table S2); Schematic representation of the experiment designs for antimicrobial activity tests (Figure S1); SEM images of enzyme-responsive fibers after degradation in various enzyme concentrations (Figure S2); SEM images of relative humidity (RH)-responsive fibers at low and high RH conditions (Figure S3); cumulative release (%) of thymol from multistimuli-responsive fibers (Figure S4) (PDF)



https://doi.org/10.1021/acsami.1c12319
ACS Appl. Mater. Interfaces 2021, 13, 50298−50308

## AUTHOR INFORMATION


### Corresponding Author

**Philip Demokritou** − *Center for Nanotechnology and Nanotoxicology, Department of Environmental Health, Harvard T. H. Chan School of Public Health, Harvard University, Boston, Massachusetts 02115, United States; School of Materials Science and Engineering, Nanyang Technological University, 639798, Singapore;* orcid.org/0000-0002-2484-9143; Email: pdemokri@hsph.harvard.edu

### Authors

**Zeynep Aytac** − *Center for Nanotechnology and Nanotoxicology, Department of Environmental Health, Harvard T. H. Chan School of Public Health, Harvard University, Boston, Massachusetts 02115, United States;* orcid.org/0000-0002-6469-9653

**Jie Xu** − *Center for Nanotechnology and Nanotoxicology, Department of Environmental Health, Harvard T. H. Chan School of Public Health, Harvard University, Boston, Massachusetts 02115, United States*

**Suresh Kumar Raman Pillai** − *School of Chemical and Biomedical Engineering, Nanyang Technological University, 637457, Singapore*

**Brian D. Eitzer** − *Department of Analytical Chemistry, The Connecticut Agricultural Experiment Station, New Haven, Connecticut 06504, United States;* orcid.org/0000-0001-7760-6893

**Tao Xu** − *Center for Nanotechnology and Nanotoxicology, Department of Environmental Health, Harvard T. H. Chan School of Public Health, Harvard University, Boston, Massachusetts 02115, United States;* orcid.org/0000-0002-1424-9363

**Nachiket Vaze** − *Center for Nanotechnology and Nanotoxicology, Department of Environmental Health, Harvard T. H. Chan School of Public Health, Harvard University, Boston, Massachusetts 02115, United States*

**Kee Woei Ng** − *Center for Nanotechnology and Nanotoxicology, Department of Environmental Health, Harvard T. H. Chan School of Public Health, Harvard University, Boston, Massachusetts 02115, United States; School of Materials Science and Engineering, Nanyang Technological University, 639798, Singapore; Environmental Chemistry and Materials Centre, Nanyang Environment and Water Research Institute, 637141, Singapore;* orcid.org/0000-0002-7276-3563

**Jason C. White** − *Department of Analytical Chemistry, The Connecticut Agricultural Experiment Station, New Haven, Connecticut 06504, United States;* orcid.org/0000-0001-5001-8143

**Mary B. Chan-Park** − *School of Chemical and Biomedical Engineering, Nanyang Technological University, 637457, Singapore;* orcid.org/0000-0003-3761-7517

**Yaguang Luo** − *Environmental Microbiology and Food Safety Laboratory, U.S. Department of Agriculture, Agricultural Research Service, Beltsville Agricultural Research Center, Beltsville, Maryland 20705, United States*

Complete contact information is available at: https://pubs.acs.org/10.1021/acsami.1c12319

### Author Contributions

[▽]Z.A. and J.X. contributed equally to this work.

### Notes

The authors declare no competing financial interest.


## ACKNOWLEDGMENTS

This research is supported by the Nanyang Technological University-Harvard T. H. Chan School of Public Health Initiative for Sustainable Nanotechnology (Project no. NTU-HSPH 18003). The characterization work was performed, in part, at the Harvard Center for Nanoscale Systems (CNS), a member of the National Nanotechnology Coordinated Infrastructure Network (NNCI), which is supported by the National Science Foundation under NSF award no. 1541959. The authors thank Wacker Chemie-AG (Michigan) and Ingredion (New Jersey) for providing cyclodextrin and starch, respectively. NV was supported by an appointment to the Agricultural Research Service (ARS) Research Participation Program administered by the Oak Ridge Institute for Science and Education (ORISE) through an interagency agreement between the U.S. Department of Energy (DOE) and the U.S. Department of Agriculture (USDA). ORISE is managed by ORAU under DOE contract number DE-SC0014664. All opinions expressed in this paper are the author's and do not necessarily reflect the policies and views of USDA, DOE, or ORAU/ORISE.

## REFERENCES


(1) Willett, W.; Rockström, J.; Loken, B.; Springmann, M.; Lang, T.; Vermeulen, S.; Garnett, T.; Tilman, D.; Declerck, F.; et al. The Lancet Commissions Food in the Anthropocene : the EAT − Lancet Commission on Healthy Diets from Sustainable Food Systems. *Lancet* **2019**, *393*, 447−492.

(2) World Health Organization (WHO). WHO Estimates of the Global Burden of Foodborne Diseases: Foodborne Disease Burden Epidemiology Reference Group 2007−2015, 2015. https://apps.who.int/iris/handle/10665/199350.

(3) Cole, M. B.; Augustin, M. A.; Robertson, M. J.; Manners, J. M. The Science of Food Security. *npj Sci. Food* **2018**, No. 14.

(4) Han, J.-w.; Luis, R.-G.; Jian-Ping, Q.; Xin-Ting, Y. Food Packaging : A Comprehensive Review and Future Trends. *Compr. Rev. Food Sci. Food Saf.* **2018**, *17*, 860−877.

(5) Siracusa, V.; Rocculi, P.; Romani, S.; Rosa, M. D. Biodegradable Polymers for Food Packaging: A Review. *Trends Food Sci Technol.* **2008**, *19*, 634−643.

(6) Senthil Muthu Kumar, T.; Senthil Kumar, K.; Rajini, N.; Siengchin, S.; Ayrilmis, N.; Varada Rajulu, A. A Comprehensive Review of Electrospun Nanofibers: Food and Packaging Perspective. *Composites, Part B* **2019**, *175*, No. 107074.

(7) Figueroa-Lopez, K. J.; Cabedo, L.; Lagaron, J. M.; Torres-Giner, S. Development of Electrospun Poly(3-hydroxybutyrate-co-3-hydroxyvalerate) Monolayers Containing Eugenol and Their Application in Multilayer Antimicrobial Food Packaging. *Front Nutr.* **2020**, *7*, No. 140.

(8) Aytac, Z.; Ipek, S.; Durgun, E.; Tekinay, T.; Uyar, T. Antibacterial Electrospun Zein Nanofibrous Web Encapsulating Thymol/Cyclodextrin-Inclusion Complex for Food Packaging. *Food Chem.* **2017**, *233*, 117−124.

(9) Aytac, Z.; Huang, R.; Vaze, N.; Xu, T.; Eitzer, B. D.; Krol, W.; MacQueen, L. A.; Chang, H.; Bousfield, D. W.; Chan-Park, M. B.; Ng, K. W.; Parker, K. K.; White, J. C.; Demokritou, P. Development of Biodegradable and Antimicrobial Electrospun Zein Fibers for Food Packaging. *ACS Sustainable Chem. Eng.* **2020**, *8*, 15354−15365.

(10) Liu, Y.; Li, Y.; Deng, L.; Zou, L.; Feng, F.; Zhang, H. Hydrophobic Ethylcellulose/Gelatin Nanofibers Containing Zinc Oxide Nanoparticles for Antimicrobial Packaging. *J. Agric. Food Chem.* **2018**, *66*, 9498.

(11) Brockgreitens, J.; Abbas, A. Responsive Food Packaging: Recent Progress and Technological Prospects. *Compr. Rev. Food Sci. Food Saf.* **2016**, *15*, 3−15.
(12) Maki, M.; Leung, K. T.; Qin, W. The Prospects of Cellulase-Producing Bacteria for the Bioconversion of Lignocellulosic Biomass. *Int. J. Biol. Sci.* **2010**, *5*, 500−516.
(13) Petruzzi, L.; Corbo, M. R.; Sinigaglia, M.; Bevilacqua, A. Microbial Spoilage of Foods: Fundamentals. *The Microbiological Quality of Food*; Woodhead Publishing, 2017.
(14) Li, Y.; Kadam, S.; Abee, T.; Slaghek, T. M.; Timmermans, J. W.; Cohen, M. A.; Norde, W.; Kleijn, M. J. Antimicrobial Lysozyme-Containing Starch Microgel to Target and Inhibit Amylase-Producing Microorganisms. *Food Hydrocolloids* **2012**, *28*, 28−35.
(15) Zelzer, M.; Todd, S. J.; Hirst, A. R.; McDonald, T. O.; Ulijn, R. V. Enzyme Responsive Materials: Design Strategies and Future Developments. *Biomater. Sci.* **2013**, *1*, 11−39.
(16) Comi, G. *Spoilage of Meat and Fish in the Microbiological Quality of Food Foodborne Spoilers*; Woodhead Publishing Series in Food Science, Technology and Nutrition, 2017; pp 179−210.
(17) Sperber, W. Introduction to the Microbiological Spoilage of Foods and Beverages. In *Compendium of the Microbiological Spoilage of Foods and Beverages*; Springer: New York, NY, 2009.
(18) Jay, J. M.; Loessner, M. J.; Golden, D. A. *Modern Food Microbiology*; Springer Science & Business Media, 2008.
(19) Del Valle, E. M. M. Cyclodextrins and Their Uses: A Review. *Process Biochem.* **2003**, *39*, 1033.
(20) Gupta, A.; Bri, S. M.; Swingler, S.; Gibson, H.; Kannappan, V.; Adamus, G.; Kowalczuk, M.; Martin, C.; Radecka, I. Synthesis of Silver Nanoparticles Using Curcumin-Cyclodextrins Loaded into Bacterial Cellulose-Based Hydrogels for Wound Dressing Applications. *Biomacromolecules* **2020**, *21*, 1802−1811.
(21) Saekhor, K.; Udomsinprasert, W.; Honsawek, S.; Tachaboonyakiat, W. Preparation of an Injectable Modified Chitosan-Based Hydrogel Approaching for Bone Tissue Engineering. *Int. J. Biol. Macromol.* **2019**, *123*, 167−173.
(22) Fuenmayor, C. A.; Mascheroni, E.; Cosio, M. S.; Piergiovanni, L.; Benedetti, S.; Ortenzi, M.; Schiraldi, A.; Mannino, S. Encapsulation of R-(+)-Limonene in Edible Electrospun Nanofibers. *Chem. Eng. Trans.* **2013**, *32*, 1771−1776.
(23) Aytac, Z.; Keskin, N. O. S.; Tekinay, T.; Uyar, T. Antioxidant $\alpha$−tocopherol/$\gamma$−cyclodextrin−inclusion complex encapsulated poly (lactic acid) electrospun nanofibrous web for food packaging. *J. Appl. Polym. Sci.* **2017**, *134*, 1−9.
(24) Pan, J.; Ai, F.; Shao, P.; Chen, H.; Gao, H. Development of Polyvinyl alcohol/$\beta$ -Cyclodextrin Antimicrobial Nanofibers for Fresh Mushroom Packaging. *Food Chem.* **2019**, *300*, 125249.
(25) Bahrami, A.; Delshadi, R.; Jafari, S. M.; Williams, L. Nanoencapsulated Nisin: An Engineered Natural Antimicrobial System for the Food Industry. *Trends Food Sci Technol.* **2019**, *94*, 20−31.
(26) Bhavaniramya, S.; Vishnupriya, S.; Al-Aboody, M. S.; Vijayakumar, R.; Baskaran, D. Role of Essential oils in Food Safety: Antimicrobial and Antioxidant Applications. *Grain Oil Sci. Technol.* **2019**, *2*, 49−55.
(27) Nemes, D.; Kovács, R.; Nagy, F.; Tóth, Z.; Herczegh, P.; Borbás, A.; Kelemen, V.; Pfliegler, W. P.; Rebenku, I.; Hajdu, P. B.; Fehér, P.; Ujhelyi, Z.; Fenyvesi, F.; Váradi, J.; Vecsernyés, M.; Bácskay, I. Comparative Biocompatibility and Antimicrobial Studies of Sorbic Acid Derivates. *Eur. J. Pharm. Sci.* **2020**, *143*, No. 105162.
(28) Uyar, T.; Hunt, M. A.; Gracz, H. S.; Tonelli, A. E. Crystalline Cyclodextrin Inclusion Compounds Formed with Aromatic Guests: Guest-Dependent Stoichiometries and Hydration-Sensitive Crystal Structures. *Cryst Growth Des.* **2006**, *6*, 1113−1119.
(29) Pyrgiotakis, G.; Luu, W.; Zhang, Z.; Vaze, N.; DeLoid, G.; Rubio, L.; Graham, W.; Adam, C.; Bell, D. C. B.; Douglas, D. P. Development of High Throughput, High Precision Synthesis Platforms and Characterization Methodologies for Toxicological Studies of Nanocellulose. *Cellulose* **2018**, *25*, 2303−2319.
(30) Bullerman, L. *Spoilage-Fungi in Food−An Overview*, 2003.
(31) El-Nemr, K. F.; Mohamed, R. M. Sorbic Acid as Friendly Curing Agent for Enhanced Properties of Ethylene Propylene Diene Monomer Rubber Using Gamma Radiation. *J. Macromol. Sci., Part A: Pure Appl.Chem.* **2017**, *54*, 711−719.
(32) Topala, C. M.; Tataru, L. D. ATR-FTIR Study of Thyme and Rosemary Oils Extracted by Supercritical Carbon Dioxide. *Rev. Chim.* **2016**, *67*, 842−846.
(33) Niaz, T.; Shabbir, S.; Noor, T.; Abbasi, R.; Raza, Z. A.; et al. Polyelectrolyte Multicomponent Colloidosomes Loaded with Nisin Z for Enhanced Antimicrobial Activity against Foodborne Resistant Pathogens. *Front Microbiol.* **2018**, *8*, 2700.
(34) Aytac, Z.; Ipek, S.; Erol, I.; Durgun, E.; Uyar, T. Fast-Dissolving Electrospun Gelatin Nanofibers Encapsulating Ciprofloxacin / Cyclodextrin Inclusion Complex. *Colloids Surf., B* **2019**, *178*, 129−136.
(35) Gao, S.; Liu, Y.; Jiang, J.; Li, X.; Ye, F.; Fu, Y.; Zhao, L. Thiram/hydroxypropyl-$\beta$-cyclodextrin inclusion complex electrospun nanofibers for a fast dissolving water-based drug delivery system. *Colloids Surf., B* **2021**, *201*, No. 111625.
(36) Nthumbi, R. M.; Ngila, J. C. Electrospun and Functionalized PVDF/PAN Nanocatalyst-Loaded Composite for Dechlorination and Photodegradation of Pesticides in Contaminated Water. *Environ. Sci. Pollut. Res.* **2016**, *23*, 20214−20231.
(37) Picciani, P. H. S.; Medeiros, E. S.; Pan, Z.; Orts, W. J.; Mattoso, L. H. C.; Soares, B. G. Development of Conducting Polyaniline / Poly ( lactic acid ) Nanofibers by Electrospinning. *J. Appl. Polym. Sci.* **2009**, *112*, 744.
(38) Kayaci, F.; Umu, O. C. O.; Tekinay, T.; Uyar, T. Antibacterial Electrospun Poly(lactic acid) (PLA) Nanofibrous Webs Incorporating Triclosan/Cyclodextrin Inclusion Complexes. *J. Agric. Food Chem.* **2013**, *61*, 3901−3908.
(39) Pimpang, P.; Sumang, R.; Choopun, S. Effect of Concentration of Citric Acid on Size and Optical Properties of Fluorescence Graphene Quantum Dots Prepared by Tuning Carbonization Degree. *Chiang Mai J. Sci.* **2018**, *45*, 2005−2014.
(40) Aytac, Z.; Yildiz, Z. I.; Kayaci-Senirmak, F.; et al. Fast-Dissolving, Prolonged Release, and Antibacterial Cyclodextrin/Limonene-Inclusion Complex Nanofibrous Webs via Polymer-Free Electrospinning. *J. Agric. Food Chem.* **2016**, *64*, 7325−7334.
(41) Zhang, Y.; Zhang, Y.; Zhu, Z.; Jiao, X.; Shang, Y.; Wen, Y. Encapsulation of Thymol in Biodegradable Nanofiber via Coaxial Electrospinning and Applications in Fruit Preservation. *J. Agric. Food Chem.* **2019**, *67*, 1736−1741.
(42) Han, D.; Sherman, S.; Filocamo, S.; Steckl, A. J. Long-Term Antimicrobial Effect of Nisin Released from Electrospun Triaxial Fiber Membranes. *Acta Biomater.* **2017**, *53*, 242−249.
(43) Saini, S.; Sillard, C.; Naceur Belgacem, M.; Bras, J. Nisin Anchored Cellulose Nanofibers for Long Term Antimicrobial Active Food Packaging. *RSC Adv.* **2016**, *6*, 12422−12430.
(44) Soto, K. M.; Hernández-Iturriaga, M.; Loarca-Piña, G.; Luna-Bárcenas, G.; Gómez-Aldapa, C. A.; Mendoza, S. Stable Nisin Food-Grade Electrospun Fibers. *J. Food Sci. Technol.* **2016**, *53*, 3787−3794.
(45) Marchese, A.; Orhan, I. E.; Daglia, M.; Barbieri, R.; Lorenzo, D.; Nabavi, S. F.; Gortzi, O.; Izadi, M.; Mohammad, S. Antibacterial and Antifungal Activities of Thymol: A Brief Review of the Literature. *Food Chem.* **2016**, *210*, 402−414.
(46) Khan, M. S. A.; Ahmad, I. Antifungal Activity of Essential Oils and Their Synergy with Fluconazole Against Drug-Resistant Strains of Aspergillus Fumigatus and Trichophyton Rubrum. *Appl Microbiol Biotechnol.* **2011**, *90*, 1083−1094.
(47) Abbaszadeh, S.; Sharifzadeh, A.; Shokri, H.; Khosravi, A. R.; Abbaszadeh, A. Antifungal Efficacy of Thymol, Carvacrol, Eugenol and Menthol as Alternative Agents to Control the Growth of Food-Relevant Fungi. *J. Mycol. Med.* **2014**, *24*, No. e51.


https://doi.org/10.1021/acsami.1c12319
ACS Appl. Mater. Interfaces 2021, 13, 50298−50308